

ResNeRF: Geometry-Guided Residual Neural Radiance Field for Indoor Scene Novel View Synthesis

Yuting Xiao¹ Yiqun Zhao¹ Yanyu Xu² Shenghua Gao¹

¹ShanghaiTech University

²Institute of High Performance Computing, and Agency for Science, Technology and Research

Abstract

We represent the ResNeRF, a novel geometry-guided two-stage framework for indoor scene novel view synthesis. Be aware of that a good geometry would greatly boost the performance of novel view synthesis, and to avoid the geometry ambiguity issue, we propose to characterize the density distribution of the scene based on a base density estimated from scene geometry and a residual density parameterized by the geometry. In the first stage, we focus on geometry reconstruction based on SDF representation, which would lead to a good geometry surface of the scene and also a sharp density. In the second stage, the residual density is learned based on the SDF learned in the first stage for encoding more details about the appearance. In this way, our method can better learn the density distribution with the geometry prior for high-fidelity novel view synthesis while preserving the 3D structures. Experiments on large-scale indoor scenes with many less-observed and textureless areas show that with the good 3D surface, our method achieves state-of-the-art performance for novel view synthesis.

1. Introduction

The emergency of metaverse technology puts forward the requirements for the scene reconstruction, especially for the indoor scenes. As high-fidelity novel view synthesis for indoor scenes with posed multi-view images would greatly reduce the costs in data acquisition, it is highly demanded in metaverse as well other AR/VR applications. However, indoor scenes usually contain lots of low-textured or textureless regions which pose great challenges for high-fidelity novel synthesis.

By far, the neural implicit representation has shown its good performance for novel view synthesis. A typical neural implicit representation utilizes the multi-layer perceptrons (MLPs) to model an object or a scene based on different representations, such as the volume density field [16] for

novel view synthesis or signed distance fields (SDF) for geometry surface reconstruction [19, 38, 42]. Although these methods have demonstrated impressive novel view synthesis performance on the object-level or local region data, the above methods might fail to generate satisfactory results when applied to large and complex indoor scenes, owing to the non-discriminative nature of these less-observed and textureless areas. These areas leads to the trivial solution for learning the density field of these areas based on the volume rendering optimization. One remedy to this issue is to use the geometry about prior of the indoor scene to regularize the optimization, and some attempts have been made along this direction. For example, researchers propose to use geometry priors such as the depth and surface normal estimated from a pretrained model [37, 44] or depth point cloud from multi-view stereo algorithms [25] as the regularizer in the objective function [7, 24] or optimization guider [39]. Their results show that this issue can be alleviated to some extent by obtaining a better surface reconstruction, while the details are still missing for novel view synthesis. The possible reason is that they only use them as geometry regularizers in the objective and enforce the correct rendering of the input views. Consequently, the geometry information may not be fully used. Then a question is natural arise: how to effectively use the geometry prior for high-fidelity novel view synthesis?

Before answering the aforementioned questions, we first need to understand the geometry ambiguity effect. To represent the scene, a branch of methods [7, 24] directly optimizing the density field with volume rendering technique for each ray without considering the geometry constraint. It indicates that the calculated depth or normal from volume rendering is inconsistency from different views. So the density distribution obtained in this way is bumpy and noisy as shown in Figure. 1. To ease this issue, a sharp density field is preferred. SDF based representation [10, 19, 37, 38, 42, 44] can meet this requirement by directly estimates the SDF and the density is transformed from SDF. These methods achieve promising surface reconstruction performance. But as the eikonal loss imposed on

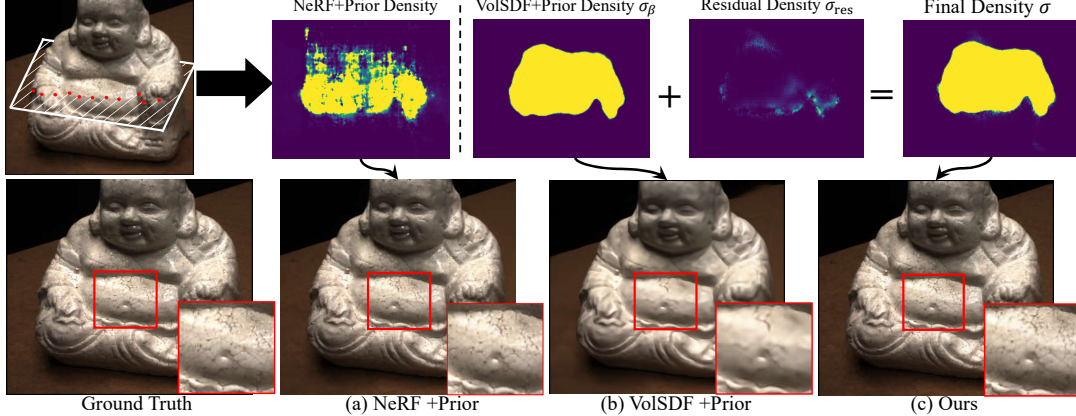


Figure 1. Illustration of the density distribution of typical novel view synthesis methods with geometry prior. We use the an object with 9 training views from DTU dataset as toy dataset for demonstration. (a) The volume density of NeRF is still noisy even if applying the geometry prior. (b) The VolSDF has smooth surface but the color appearance is not detailed enough. (c) The geometry-guided residual density of our method can attach to the surface and generate fine color appearance detail.

SDF and the transformation from SDF to density constraining the flexibility of the density field in volume rendering, some details of appearance in novel synthesis are missing.

As aforementioned, geometry based representation can provides a prior about the density distribution. To fully use the geometry prior about the scene and increases the flexibility in optimizing density field for better novel view synthesis, in this paper, we propose a novel geometry-guided two-stage framework for indoor scene novel view synthesis, which consists a geometry optimization stage for learning a good SDF representation, and an appearance details optimization stage by learning the density residual based on geometry learned in the first stage. To be specific, in the geometry optimization stage, we aims to obtain a fine surface and a coarse color appearance. Following the VolSDF [42] and other related works [10, 37, 44] with geometry prior, we apply the SDF with eikonal loss function and geometry prior to optimize the geometry representation. This would lead to a good geometry reconstruction, which would avoid the geometry ambiguity to some extent. After the training of the first stage, the geometry represented as SDF is fixed. In the appearance details optimization stage, we aim to obtain finer details in appearance with the the geometry surface. In particular, we design the geometry-guided residual density field to refine the density field transformed from SDF, which would enhance the details in appearance for better novel view synthesis. As shown in Figure 1 (c), the geometry guidance can ensure the residual density generated near the geometry surface and the appearance is significantly improved with more details. As a geometry-guided density residual is learned in our framework, we term our method as ResNeRF. We evaluate our ResNeRF for novel view synthesis on ScanNet and Tanks and Temples which are large scale indoor scenes datasets. Experimental results show that

our method generates high-fidelity novel-view synthesis results while preserving good surface.

Our contributions of our work can be summarized as followings: i)We propose ResNeRF, a geometry-guided two-stage framework for indoor scene novel view synthesis. By inheriting the results of SDF based geometry reconstruction in the first stage, our method can better synthesize the novel views while preserving a good geometry. ii) We introduce a SDF based density residual learning that can better leverage the geometry prior and reduce the influence of geometry ambiguity, consequently improves the novel view synthesis. iii) Experimental results on large scale indoor datasets show that our ResNeRF achieves state-of-the-art performance for novel view synthesis performance.

2. Related Work

Neural Radiance Fields. Implicit volumetric representations have been widely developed for 3D novel view synthesis. The NeRF [16] applies an MLP as the coordinate-based implicit contiguous function to model the volume density and view-dependent color information. Then more researchers applied the volume rendering technique to render the images for the target viewpoints and found out that only using high-frequency representation capacity in NeRF might not be sufficient. Thus, there occur some works [29, 33] , adopting the position encoding operation with different frequency to NeRF for further improvement. Many works follow this framework and improve it in many aspects, such as model acceleration [17, 31], compression [5, 23, 32], and relighting [3, 30, 36]. And various 3D-related tasks adopt this approach such as scene decomposition and editing [40, 41] and dynamic modeling [15, 20].

3D Reconstruction from Multi-view Image. The 3D ge-

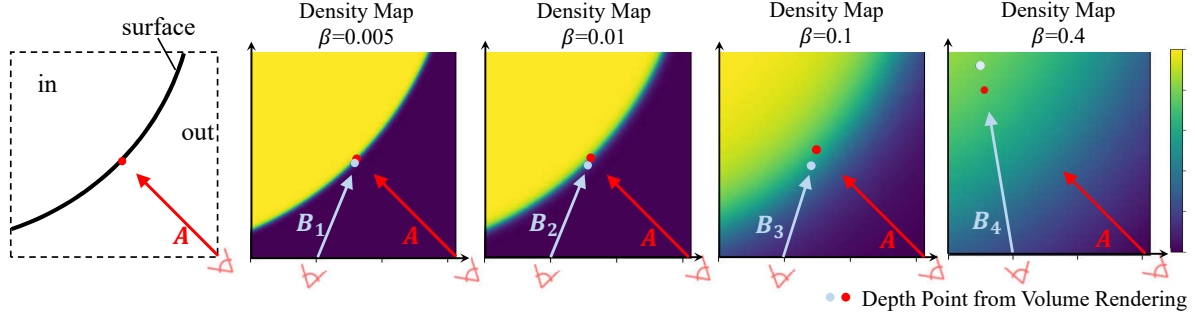


Figure 2. **Geometry Ambiguity.** A ray \mathbf{r}_A intersects at a point on the surface and the depth point of this ray \mathbf{r}_A can be computed by volume rendering technique (Eq3). Another ray \mathbf{r}_B casts to this depth point (Red dot) from another viewpoint. The depth points of two rays computed from volume rendering cannot be guaranteed to be consistent unless the volume density is sharp and large enough near the surface. It indicates that the geometry regularization at the training views cannot be generalized to novel views well unless the density field is sharp and large enough near the surface.

ometry reconstruction from multi-view images is a fundamental and important task in computer vision and has developed for a long time. Traditional multi-view stereo algorithms focus on the 3D space feature matching [1, 2, 4, 6] based on the geometry relationship or the explicit shape representation design [28, 34, 35]. Then some learning-based methods are proposed to involve the deep neural networks to replace some steps which are tough for mathematical modeling, such as depth estimation [11, 27], feature extraction, and feature matching [13, 14]. Recently, instead of utilizing the explicit representation, many works [18, 43] use the neural implicit network for geometry shape representation, such as MLP, which achieves impressive reconstruction results. An important advantage of neural implicit representation is that the contiguous modeling can generate a smooth surface without the noisy floats. Following the volume rendering method in NeRF [16], some works [19, 38, 42] transform the SDF representation to volume density representation for rendering RGB images, which can apply the multi-view images as supervision without the requirement of the mask.

Prior for 3D reconstruction. Since the less-observed and textureless area is ubiquitous in a large indoor scene, only applying the multi-view images as supervision is absolutely not enough for Multi-view Stereo. Some methods [10, 24, 37, 39, 44] apply the geometry prior such as depth, normal, and point cloud to improve the results. And the semantic prior [40, 45] is also a useful choice in this task.

In this work, we propose a novel approach to utilize the geometry prior as guidance to enhance the performance for both 3D reconstruction and novel view synthesis. Instead of directly applying the geometry prior as regularizer [7, 24, 39] in NeRF, we apply the monocular geometry prior on the first geometry optimization stage and using the obtained SDF as guidance to the second color appearance stage.

3. Method

In this work, we focus on the novel view synthesis for the large-scale indoor scene with geometry prior. We first introduce the geometry ambiguity problem when applying geometry prior in the volume rendering technique. After that, we present a new two-stages framework using the monocular geometry priors. The first geometry optimization stage applies the SDF representation to obtain the surface, while the second appearance details optimization stage applies the parameterized residual density with the obtained geometry surface as guidance for better novel view rendering.

3.1. Geometry Ambiguity

In this part, we introduce the geometry ambiguity, indicating that the geometry such as the depth and normal calculated from volume density rendering is inconsistency from different view points. This problem could make the regularization of depth and normal from the training view cannot be generalized to the novel views very well. Especially for the large scale indoor scene, the less-observed and textureless region make the using of geometry prior insufficiently.

The volume rendering technique represents the static scene as the volume density and the directional emitted color at each point in the space. In particular, the rendered color of a ray $\mathbf{r}(t) = \mathbf{o} + t\mathbf{d}$ in the space is:

$$\hat{\mathbf{C}}(\mathbf{r}) = \sum_{i=1}^N T_i \alpha_i \mathbf{c}_i, \quad (1)$$

where T_i and α_i denote the transparency and alpha value at the i^{th} point on the ray \mathbf{r} , respectively:

$$T_i = \prod_{j=1}^{i-1} (1 - \alpha_j), \quad \alpha_i = 1 - \exp(-\sigma_{\beta i} \delta_i) \quad (2)$$

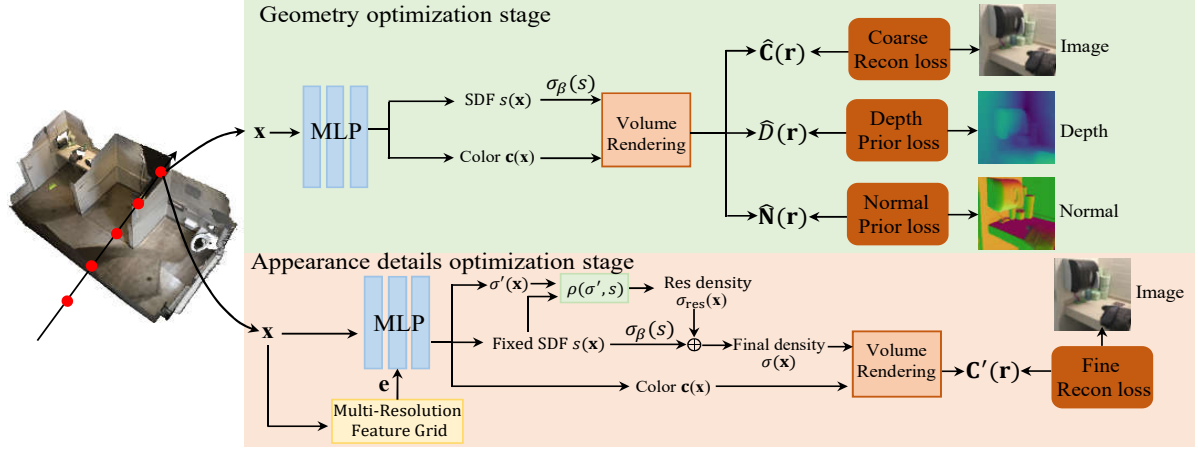


Figure 3. The overview of our geometry guided two-stage model. Our model first optimizes geometry to obtain fine geometry representation and coarse color appearance and second focus on the appearance detail refinement. The depth and normal prior are provided by the pretrained Omnidata model [8].

The depth and normal can be computed as:

$$\hat{D}(\mathbf{r}) = \sum_{i=1}^N T_i \alpha_i t_i \quad \hat{\mathbf{N}}(\mathbf{r}) = \sum_{i=1}^N T_i \alpha_i \mathbf{n}_i \quad (3)$$

where the t_i and \mathbf{n}_i is the distance to camera and the gradient of i^{th} point on ray \mathbf{r} .

We qualitatively demonstrate the geometry ambiguity problem in Figure 2. Since the volume density distribution does not meet any mathematical constraints, we apply the transformation function from SDF to density in VolSDF [42] as the formulation to qualitatively explain and demonstrate this problem. Besides, geometry ambiguity would be more serious for density field in NeRF [16] based methods [7, 24, 39] due to lacking geometry constraints.

Suppose there is a circle surface, we transform the SDF to density values σ_β , following the implementation of VolSDF [42]:

$$\sigma_\beta(s) = \begin{cases} \frac{1}{2\beta} \exp\left(\frac{s}{\beta}\right) & \text{if } s \leq 0 \\ \frac{1}{\beta} - \frac{1}{2\beta} \exp\left(-\frac{s}{\beta}\right) & \text{if } s > 0 \end{cases} \quad (4)$$

where the β is a learnable parameter. As proved in VolSDF, β would gradually decrease in the optimization.

A ray $\mathbf{r}_A = \mathbf{o}_A + t\mathbf{d}_A$ hits on a circular surface and the depth point of this ray can be calculated by volume rendering. And another ray $\mathbf{r}_B = \mathbf{o}_B + t\mathbf{d}_B$ from another view passes through the depth point of \mathbf{r}_A , which is computed by volume rendering technique. If the geometry is consistent from different views, the depth point of ray \mathbf{r}_B should be the same as the depth point of ray \mathbf{r}_A . However, We observe that the geometry depth can not keep consistent unless the volume density field is sharp and large enough at inside. Otherwise, the depth points of two rays cannot be

consistent, which means:

$$\mathbf{o}_1 + \hat{D}(\mathbf{r}_1)\mathbf{d}_1 \neq \mathbf{o}_2 + \hat{D}(\mathbf{r}_2)\mathbf{d}_2 \quad (5)$$

And the normal also suffer from the same struggle:

$$\hat{\mathbf{N}}(\mathbf{r}_1) \neq \hat{\mathbf{N}}(\mathbf{r}_2) \quad (6)$$

The volume density representation does not have a defined level set corresponding to the surface, so the geometry ambiguity problem makes the regularization of geometry prior to different views insufficient. Especially for the less-observed region, only applying the geometry prior as a regularizer in loss function cannot provide efficient regularization. So, the sharp and sufficiently large volume density field is necessary for applying geometry prior.

Based on the aforementioned analysis, we observe that previous SDF-based methods such as VolSDF [42] can satisfy this requirement. However, directly applying the geometry prior to these methods cannot obtain high novel view rendering quality because of the joint optimization and single 3D geometry modeling problem mentioned before. To solve these problems, we propose to utilize a two-stage framework, which firstly focuses on the surface reconstruction to obtain a sharp volume density field and secondly learns a residual density field by using geometry guidance for refinement.

3.2. Geometry Optimization Stage

In this stage, our method mainly aims to obtain good 3D reconstruction results and coarse color appearance by applying the geometry prior. We follow the previous works [19, 38, 42] optimizing the surface represented by the implicit neural network via the image reconstruction loss. For each pixel on the image corresponding to a ray \mathbf{r} , M points

$\mathbf{x} = \mathbf{o} + t\mathbf{d}$ are sampled on each ray and the SDF s , and color values $\hat{\mathbf{C}}(\mathbf{r})$ are predicted. N rays are sampled.

The loss function of this geometry optimization stage has these terms:

Coarse Reconstruction Loss. We utilize the Eq(1) to compute the predicted RGB image observation and apply the posed training images as supervision:

$$\mathcal{L}_{\text{rgb}} = \frac{1}{N} \sum_{\mathbf{r} \in \mathcal{R}} \|\hat{\mathbf{C}}(\mathbf{r}) - \mathbf{C}(\mathbf{r})\|_1 \quad (7)$$

Eikonal Loss. Following the typical method, the Eikonal loss is applied to regularize the SDF of the scene:

$$\mathcal{L}_{\text{eik}} = \frac{1}{MN} \sum_{\mathbf{x} \in \mathcal{X}} (\|\nabla f_{\theta}(\mathbf{x})\|_2 - 1)^2 \quad (8)$$

Geometry Prior Loss. About utilizing geometry prior, following the previous works [44], we adopt the geometry prior loss as these two terms:

$$\mathcal{L}_{\text{depth}} = \frac{1}{N} \sum_{\mathbf{r} \in \mathcal{R}} \|w(\hat{D}(\mathbf{r}) + b) - D(\mathbf{r})\|^2 \quad (9)$$

$$\mathcal{L}_{\text{norm}} = \frac{1}{N} \sum_{\mathbf{r} \in \mathcal{R}} \|\hat{\mathbf{N}}(\mathbf{r}) - \mathbf{N}(\mathbf{r})\|_1 + \|1 - \hat{\mathbf{N}}(\mathbf{r})^T \mathbf{N}(\mathbf{r})\|_1 \quad (10)$$

where the w and b are the scale and shift to match the depth prediction and depth prior since the depth prior generated by pretrained model is not the depth in the real world, it is only up to scale. The factor w and b are estimated individually per image with a least-squares criterion, which is the same as [9, 22, 44]. Besides, the approach for using geometry prior can also follow other works such as [10, 37].

The total loss function in the geometry optimization stage for focusing on geometry optimization is:

$$\mathcal{L}_{\text{geo}} = \mathcal{L}_{\text{rgb}} + \lambda_1 \mathcal{L}_{\text{eik}} + \lambda_2 \mathcal{L}_{\text{depth}} + \lambda_3 \mathcal{L}_{\text{norm}} \quad (11)$$

3.3. Appearance Details Optimization Stage

After the optimization of geometry optimization stage, we can obtain the geometry surface of the scene. In this appearance details optimization stage, we aim to refine the volume density and color appearance near the surface by applying the SDF obtained from the geometry optimization stage as guidance. It can be considered that the geometry prior is converted to the SDF representation which does not suffer from geometry ambiguity in this stage. We fix the parameters of the implicit neural network corresponding to SDF representation in the geometry optimization stage.

We define the final fine volume density of the point \mathbf{x} as the combination of the base density from SDF and the residual density:

$$\sigma(\mathbf{x}) = \sigma_{\beta}(s(\mathbf{x})) + \sigma_{\text{res}}(\mathbf{x}) \quad (12)$$

The residual density could be considered as the refinement of the base density obtained from the transformation of SDF. As it does not need to be constrained by the eikonal loss and the transformation from SDF to density, the residual density has more flexibility than the base density. Besides, we consider that the residual density field should mainly modify and refine the base density near the surface, so the residual density is designed as:

$$\sigma_{\text{res}}(\mathbf{x}) = \rho(\sigma'(\mathbf{x}), s(\mathbf{x})) = \omega(s(\mathbf{x})) \cdot \sigma'(\mathbf{x}) \quad (13)$$

where the weight $\omega(s) = \exp(-a|s|)$, the a is a hyper-parameter.

Similar to the geometry optimization stage, the color prediction in this appearance details optimization stage is defined as follows:

$$T'{}_i = \prod_{j=1}^{i-1} (1 - \alpha'_j) \quad \alpha'_i = 1 - \exp(-\sigma_i \delta_i) \quad (14)$$

$$\mathbf{C}'(\mathbf{r}) = \sum_{i=1}^N T'{}_i \alpha'_i \mathbf{c}_i \quad (15)$$

Fine Reconstruction Loss. We only apply the color reconstruction loss in the second stage which focuses on learning fine color appearance representation:

$$\mathcal{L}_{\text{color}} = \frac{1}{N} \sum_{\mathbf{r} \in \mathcal{R}} \|\mathbf{C}'(\mathbf{r}) - \mathbf{C}(\mathbf{r})\|_2^2 \quad (16)$$

3.4. Color Representation Enhancement.

Most of the geometry surface of the indoor scene is just a simple plane, such as wall, floor, and table, which is suitable to apply contiguous representations such as MLP for modeling. This is verified in [44]. But the color appearance consists of a much more diverse high-frequency signal, which is reasonable to apply discrete representation such as the multi-resolution feature grid for modeling.

In the geometry optimization stage, we use the MLP to represent the geometry SDF network f_{θ} and color network \mathbf{c}_{θ} :

$$(s, \mathbf{z}) = f_{\theta}(\mathbf{x}) \quad \mathbf{c} = \mathbf{c}_{\theta}(\mathbf{x}, \mathbf{d}, \mathbf{z}, \mathbf{0}) \quad (17)$$

where the \mathbf{z} is the latent vector and the $\mathbf{0}$ is the zero vector.

And in the appearance details optimization stage, with geometry network f_{θ} fixed, we apply the multi-resolution feature grid [17] to enhance the capacity of representing color appearance and σ' for residual density field and color appearance. Suppose the \mathbf{e} is the feature vector computed by the interpolation from multi-resolution feature grid:

$$\mathbf{c} = \mathbf{c}_{\theta}(\mathbf{x}, \mathbf{d}, \mathbf{z}, \mathbf{e}) \quad (18)$$

$$\sigma' = \sigma_{\theta}(\mathbf{x}, \mathbf{e}) \quad (19)$$

Method	scene 0616		scene 0521		scene 0000		scene 0158	
	PSNR	SSIM	PSNR	SSIM	PSNR	SSIM	PSNR	SSIM
NeRF [16]	24.80	0.7775	30.16	0.8207	26.30	0.7744	29.64	0.8717
NeRF+Prior	21.94	0.7010	28.93	0.7894	23.34	0.6927	27.67	0.8391
NerfingMVS [39]	18.94	0.5956	25.96	0.7178	24.15	0.7517	24.56	0.7825
DDPNeRF [24]	23.99	0.7824	30.36	0.7794	25.74	0.7625	29.52	0.8106
ResNeRF	25.78	0.8160	31.07	0.8552	27.10	0.8274	30.75	0.9070

Method	scene 0316		scene 0553		scene 0653		scene 0079	
	PSNR	SSIM	PSNR	SSIM	PSNR	SSIM	PSNR	SSIM
NeRF [16]	26.71	0.8740	32.45	0.9151	25.07	0.7922	27.89	0.7902
NeRF+Prior	26.72	0.8797	31.66	0.9087	25.20	0.8045	24.30	0.6803
NerfingMVS [39]	23.77	0.7311	27.06	0.8381	21.21	0.7093	22.18	0.6322
DDPNeRF [24]	26.46	0.7912	30.34	0.8796	25.69	0.8024	27.36	0.7774
ResNeRF	27.94	0.9065	33.02	0.935	26.82	0.8592	28.64	0.8327

Table 1. The comparative experiments with other baselines on the ScanNet dataset. Our method achieve state-of-the-art performance, especially on SSIM, which indicates better geometry structure representation

Method	Courtroom		Auditorium		Museum		Ballroom	
	PSNR	SSIM	PSNR	SSIM	PSNR	SSIM	PSNR	SSIM
NeRF [16]	21.14	0.6252	23.90	0.8133	19.45	0.5963	24.48	0.7093
NeRF+Prior	22.55	0.7020	24.21	0.8189	19.73	0.6121	24.20	0.7225
NerfingMVS [39]	19.77	0.4376	21.95	0.5597	18.62	0.3594	16.88	0.2907
ResNeRF	23.03	0.7714	24.63	0.8652	20.47	0.7212	25.40	0.8221

Table 2. The comparative experiments with other baselines on the Tanks and Temples dataset. It proves the efficiency of our method.

We use the multi-resolution feature grid instead of dense or single resolution grid because we default this is the best solution in grid based approach. We investigate ablation studies to explain why this enhancement is not applied in geometry optimization stage.

4. Experiments

4.1. Experimental Setup

We implement our model on PyTorch platform [21]. In our implementation, we train our model for 200K iterations on each scene with the first 160K for the geometry optimization stage and the last 40K for the appearance details optimization stage. We use the Adam optimizer [12] with a learning rate of 5e-4 for neural networks and 1e-2 for multi-resolution feature grids. The hyper-parameter a for residual density optimization is set to 10. The depth and normal prior are provided by the pretrained Omnidata model [8]. The experiments are implemented on one NVIDIA TITAN V GPU. The images are resized to 384×384 .

Datasets. The main goal of this work is to the more complex and challenging global scenes for performance comparison, unlike the commonly used datasets in the geometry prior based works, the novel view synthesis at a local region of the indoor scene using small camera movement. Thus,

we use the large indoor scene dataset ScanNet and Tanks and Temples advanced sets to evaluate the effectiveness of our method. For ScanNet, we uniformly sample 1/10 of all the views for training. Both datasets are randomly sampled 30 views for the test.

Baselines. We compare our method with the following methods: The state-of-the-art methods for the large-scale indoor scene: NeRF [16] learns the neural radiance field with and without prior; NerfingMVS [39] and DDP-NeRF [24] applies depth prior as optimization guider or regularizer. The state-of-the-art 3D reconstruction works: UNISURF [19], VoISDF [42], Neus [38], Manhattan-SDF [10], NeuRIS [37] and MonoSDF [44].

Metrics. We use the four commonly used metrics, including PSNR, SSIM, Chamfer Distance, and the F-score, to evaluate our method and baselines for novel view synthesis. PSNR focuses on the quality of rendered pixel color, while the SSIM focuses on the quality of geometry edges and high-frequency texture. Besides, the Chamfer Distance and the F-score with a threshold of 5cm is used to evaluate the 3D reconstruction results.

4.2. Performance Comparisons

We conduct the experiments on two large-scale indoor scene datasets to compare our method with other baselines

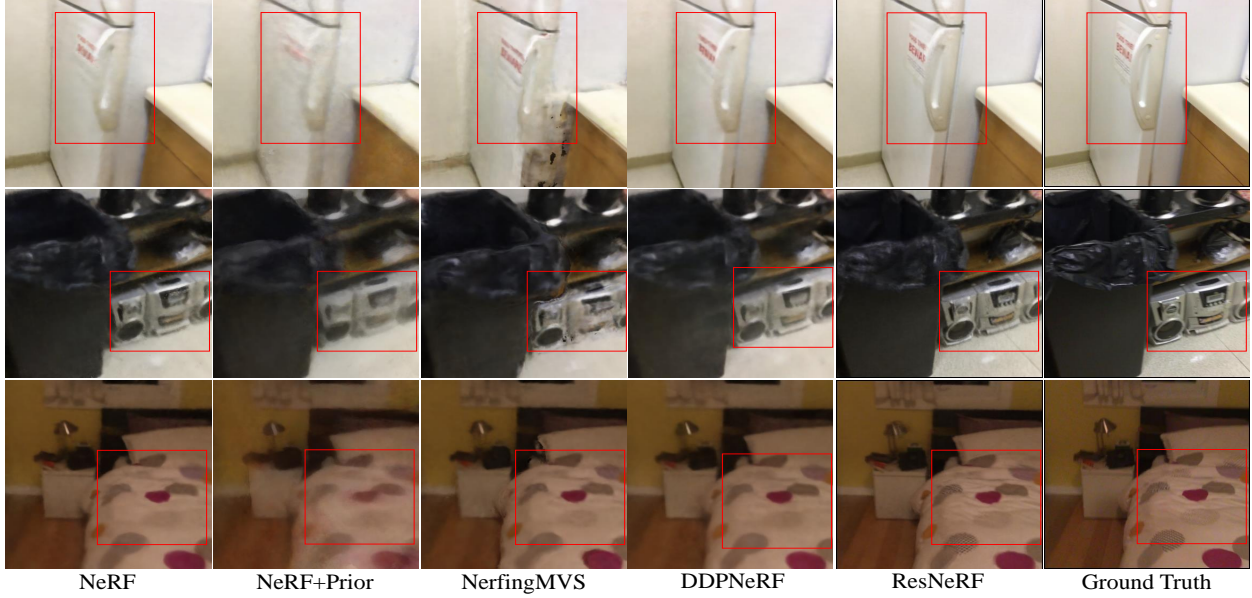


Figure 4. The qualitative results of our method and other baselines. Our method can generate more detailed appearance with clear geometry structure than other baselines.

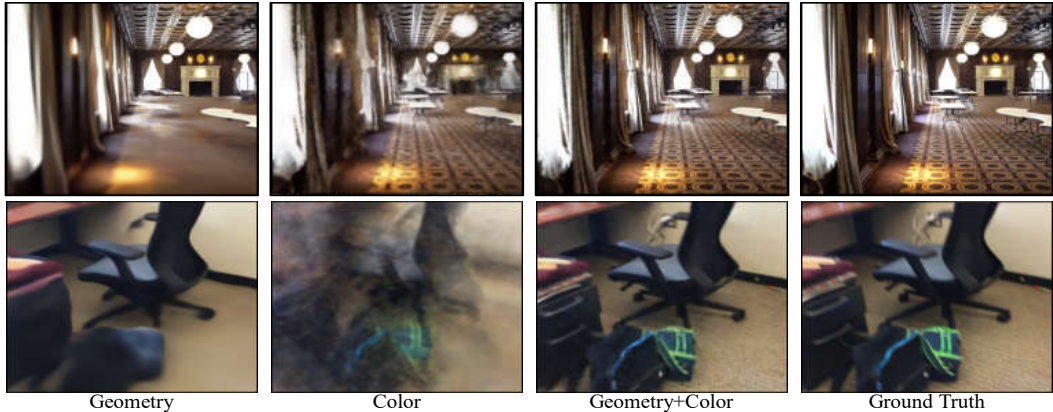


Figure 5. The qualitative ablation study of two-stage design. Only applying the geometry optimization stage cannot generate detailed appearance. Only applying the appearance details optimization stage cannot preserve the geometry structure information.

ScanNet Dataset. We compare our model with existing methods for novel view synthesis on indoor scenes. The quantitative experiments are shown in Table 1. The NeRF + Prior indicates applying the same pretrained Omnidata [8] geometry prior as our method in the first geometry optimization stage. We find that the improvement of using the geometry prior from COLMAP or pretrained model is limited. And it can be observed that our method can achieve better performance than existing works. And we observe that our method can obtain significantly higher SSIM which is more focus on the geometry edge and texture of the rendered images. This indicates that our image can generate novel view images with more edge and bound details.

Tanks and Temples Dataset. The Tanks and Temples advanced sets is obviously larger and more complex than ScanNet. The quantitative experiments are shown in Table 2. We can observe that our method can achieve impressive improvement on large-scale datasets.

The qualitative results are shown in Figure. 4. It can be observe that our method outperform other baselines with more detailed appearance.

Scene Reconstruction. We also evaluate the 3D scene surface reconstruction performance of our method, which is shown in Table 3. Compared with existing state-of-the-art baselines, our method can achieve comparable performance with previous works. It indicates that our method can also

Method	COLMAP [26]	NeuS [38]	VolSDF [42]	M-SDF [10]	NeuRIS [37]	MonoSDF [44]	Ours
Chamfer- L_1	0.141	0.194	0.267	0.070	0.050	0.042	0.042
F-score	0.537	0.291	0.364	0.602	0.692	0.733	0.730

Table 3. The performance comparison on 3D reconstruction on ScanNet dataset. Our method can achieve comparable performance to the previous state-of-the-art methods for 3D surface reconstruction.

Stage	ScanNet		TNT	
	PSNR	SSIM	SSIM	PSNR
Geometry	25.91	0.8332	21.48	0.6889
Color	24.92	0.8084	19.78	0.6254
Geometry+Color	28.90	0.8675	23.52	0.7982

Table 4. Ablation study for two-stage design. This proves the effectiveness of the two-stage design. individually focusing on the geometry and color appearance is significant.

achieve good 3D geometry reconstruction performance.

4.3. Ablation Studies

In this subsection, we conduct ablation studies to evaluate the efficiency of the two-stages design and the color appearance enhancement.

Two-stages Design. To investigate the effectiveness of our designed two-stage framework, we design the following baselines. The first one only applies the geometry optimization stage, denoted as ‘*Geometry*’, removing the residual density representation. The second one applies the appearance details optimization stage, denoted as ‘*Color*’, optimizing the residual density based on the randomly initialized geometry guidance. The results are shown in Table 4. The large gaps indicate the effectiveness of the proposed two-stage design. In particular, the two-stage design could optimize the base density from SDF and the residual density in the geometry and appearance details optimization stage respectively, to avoid the geometry ambiguity problems and achieve promising improvement.

The qualitative results are shown in Figure. 5. Compare with the results obtained from only the geometry optimization stage, our model can synthesize detailed color appearance. This proves that the residual density can improve the capacity for representing appearance details. Besides, The results obtained from only the appearance details optimization stage are pretty noisy, which indicates the efficiency of geometry guidance.

Color Representation Enhancement. To indicate the effectiveness of the used color representation enhancement by multi-resolution feature grid. The experimental results are shown in Table 5. We design a baseline not applying the multi-resolution feature grid corresponding to the first row at Table 5. The second row indicates we concatenate the

Geometry	Color	ScanNet	
		PSNR	SSIM
None	None	28.31	0.8557
Grids	None	27.01	0.8319
None	Grids	28.90	0.8675
Grids	Grids	27.62	0.8427

Table 5. Ablation studies for color representation enhancement in appearance details optimization stage. This results indicates only applying the multi-resolution feature grid to the appearance details optimization stage is better than other choices.

feature from multi-resolution grid to the input of the geometry network, residual density network, and color network. The third row corresponds to our method, the feature from multi-resolution feature grid is only concatenated to the input of the residual density network and color network in the appearance details optimization stage.

We can see that the baseline with the color representation enhancement outperforms the one without the color representation enhancement. The potential reason is that applying the multi-resolution feature grid would enlarge the capacity of color appearance representation, and too strong color representation at the geometry optimization stage would reduce the performance. The potential reason is that too strong color appearance capacity is unfavorable to geometry reconstruction since this would lock the geometry optimization in the local optimum. So the enhancement with multi-resolution feature grid should be applied in the geometry optimization stage.

5. Conclusion

In this work, we propose ResNeRF, a new approach that mainly focuses on novel view synthesis with geometry prior of the indoor scene. The indoor scene contains much less-observed and textureless region, which leads to serious geometry ambiguity problem for NeRF-based methods [7, 24, 39], and this makes the use of geometry prior insufficient. The ResNeRF develops a two-stage framework representing the scene as SDF, residual density field and color appearance, which avoids the geometry ambiguity problem. We believe this framework can utilize geometry prior more sufficiently for novel view synthesis.

References

[1] Motilal Agrawal and Larry S Davis. A probabilistic framework for surface reconstruction from multiple images. In *Proceedings of the 2001 IEEE Computer Society Conference on Computer Vision and Pattern Recognition. CVPR 2001*, volume 2, pages II–II. IEEE, 2001. 3

[2] Michael Bleyer, Christoph Rhemann, and Carsten Rother. Patchmatch stereo-stereo matching with slanted support windows. In *Bmvc*, volume 11, pages 1–11, 2011. 3

[3] Mark Boss, Raphael Braun, Varun Jampani, Jonathan T Barron, Ce Liu, and Hendrik Lensch. Nerd: Neural reflectance decomposition from image collections. In *Proceedings of the IEEE/CVF International Conference on Computer Vision*, pages 12684–12694, 2021. 2

[4] Adrian Broadhurst, Tom W Drummond, and Roberto Cipolla. A probabilistic framework for space carving. In *Proceedings eighth IEEE international conference on computer vision. ICCV 2001*, volume 1, pages 388–393. IEEE, 2001. 3

[5] Anpei Chen, Zexiang Xu, Andreas Geiger, Jingyi Yu, and Hao Su. Tensorf: Tensorial radiance fields. *arXiv preprint arXiv:2203.09517*, 2022. 2

[6] Jeremy S De Bonet and Paul Viola. Poxels: Probabilistic voxelized volume reconstruction. In *Proceedings of International Conference on Computer Vision (ICCV)*, volume 2, 1999. 3

[7] Kangle Deng, Andrew Liu, Jun-Yan Zhu, and Deva Ramanan. Depth-supervised nerf: Fewer views and faster training for free. In *Proceedings of the IEEE/CVF Conference on Computer Vision and Pattern Recognition*, pages 12882–12891, 2022. 1, 3, 4, 8

[8] Ainaz Eftekhar, Alexander Sax, Jitendra Malik, and Amir Zamir. Omnidata: A scalable pipeline for making multi-task mid-level vision datasets from 3d scans. In *Proceedings of the IEEE/CVF International Conference on Computer Vision*, pages 10786–10796, 2021. 4, 6, 7

[9] David Eigen, Christian Puhrsch, and Rob Fergus. Depth map prediction from a single image using a multi-scale deep network. *Advances in neural information processing systems*, 27, 2014. 5

[10] Haoyu Guo, Sida Peng, Haotong Lin, Qianqian Wang, Guofeng Zhang, Hujun Bao, and Xiaowei Zhou. Neural 3d scene reconstruction with the manhattan-world assumption. In *Proceedings of the IEEE/CVF Conference on Computer Vision and Pattern Recognition*, pages 5511–5520, 2022. 1, 2, 3, 5, 6, 8

[11] Po-Han Huang, Kevin Matzen, Johannes Kopf, Narendra Ahuja, and Jia-Bin Huang. Deepmvs: Learning multi-view stereopsis. In *Proceedings of the IEEE Conference on Computer Vision and Pattern Recognition*, pages 2821–2830, 2018. 3

[12] Diederik P Kingma and Jimmy Ba. Adam: A method for stochastic optimization. *arXiv preprint arXiv:1412.6980*, 2014. 6

[13] Vincent Leroy, Jean-Sébastien Franco, and Edmond Boyer. Shape reconstruction using volume sweeping and learned photoconsistency. In *Proceedings of the European Conference on Computer Vision (ECCV)*, pages 781–796, 2018. 3

[14] Wenjie Luo, Alexander G Schwing, and Raquel Urtasun. Efficient deep learning for stereo matching. In *Proceedings of the IEEE conference on computer vision and pattern recognition*, pages 5695–5703, 2016. 3

[15] Ricardo Martin-Brualla, Noha Radwan, Mehdi SM Sajjadi, Jonathan T Barron, Alexey Dosovitskiy, and Daniel Duckworth. Nerf in the wild: Neural radiance fields for unconstrained photo collections. In *Proceedings of the IEEE/CVF Conference on Computer Vision and Pattern Recognition*, pages 7210–7219, 2021. 2

[16] Ben Mildenhall, Pratul P Srinivasan, Matthew Tancik, Jonathan T Barron, Ravi Ramamoorthi, and Ren Ng. Nerf: Representing scenes as neural radiance fields for view synthesis. *Communications of the ACM*, 65(1):99–106, 2021. 1, 2, 3, 4, 6

[17] Thomas Müller, Alex Evans, Christoph Schied, and Alexander Keller. Instant neural graphics primitives with a multiresolution hash encoding. *arXiv preprint arXiv:2201.05989*, 2022. 2, 5

[18] Michael Niemeyer, Lars Mescheder, Michael Oechsle, and Andreas Geiger. Differentiable volumetric rendering: Learning implicit 3d representations without 3d supervision. In *Proceedings of the IEEE/CVF Conference on Computer Vision and Pattern Recognition*, pages 3504–3515, 2020. 3

[19] Michael Oechsle, Songyou Peng, and Andreas Geiger. Unisurf: Unifying neural implicit surfaces and radiance fields for multi-view reconstruction. In *Proceedings of the IEEE/CVF International Conference on Computer Vision*, pages 5589–5599, 2021. 1, 3, 4, 6

[20] Keunhong Park, Utkarsh Sinha, Jonathan T Barron, Sofien Bouaziz, Dan B Goldman, Steven M Seitz, and Ricardo Martin-Brualla. Nerfies: Deformable neural radiance fields. In *Proceedings of the IEEE/CVF International Conference on Computer Vision*, pages 5865–5874, 2021. 2

[21] Adam Paszke, Sam Gross, Francisco Massa, Adam Lerer, James Bradbury, Gregory Chanan, Trevor Killeen, Zeming Lin, Natalia Gimelshein, Luca Antiga, Alban Desmaison, Andreas Kopf, Edward Yang, Zachary DeVito, Martin Raison, Alykhan Tejani, Sasank Chilamkurthy, Benoit Steiner, Lu Fang, Junjie Bai, and Soumith Chintala. Pytorch: An imperative style, high-performance deep learning library. In H. Wallach, H. Larochelle, A. Beygelzimer, F. d'Alché-Buc, E. Fox, and R. Garnett, editors, *Advances in Neural Information Processing Systems 32*, pages 8024–8035. Curran Associates, Inc., 2019. 6

[22] René Ranftl, Katrin Lasinger, David Hafner, Konrad Schindler, and Vladlen Koltun. Towards robust monocular depth estimation: Mixing datasets for zero-shot cross-dataset transfer. *IEEE transactions on pattern analysis and machine intelligence*, 2020. 5

[23] Daniel Rebain, Wei Jiang, Soroosh Yazdani, Ke Li, Kwang Moo Yi, and Andrea Tagliasacchi. Derf: Decomposed radiance fields. In *Proceedings of the IEEE/CVF Conference on Computer Vision and Pattern Recognition*, pages 14153–14161, 2021. 2

[24] Barbara Roessle, Jonathan T Barron, Ben Mildenhall, Pratul P Srinivasan, and Matthias Nießner. Dense depth priors for neural radiance fields from sparse input views. In *Proceedings of the IEEE/CVF Conference on Computer Vision and Pattern Recognition*, pages 12892–12901, 2022. [1](#), [3](#), [4](#), [6](#), [8](#)

[25] Johannes L Schonberger and Jan-Michael Frahm. Structure-from-motion revisited. In *Proceedings of the IEEE conference on computer vision and pattern recognition*, pages 4104–4113, 2016. [1](#)

[26] Johannes L Schönberger, Enliang Zheng, Jan-Michael Frahm, and Marc Pollefeys. Pixelwise view selection for unstructured multi-view stereo. In *European conference on computer vision*, pages 501–518. Springer, 2016. [8](#)

[27] Johannes Lutz Schönberger, Enliang Zheng, Marc Pollefeys, and Jan-Michael Frahm. Pixelwise view selection for unstructured multi-view stereo. In *European Conference on Computer Vision (ECCV)*, 2016. [3](#)

[28] Steven M Seitz and Charles R Dyer. Photorealistic scene reconstruction by voxel coloring. *International Journal of Computer Vision*, 35(2):151–173, 1999. [3](#)

[29] Vincent Sitzmann, Julien Martel, Alexander Bergman, David Lindell, and Gordon Wetzstein. Implicit neural representations with periodic activation functions. *Advances in Neural Information Processing Systems*, 33:7462–7473, 2020. [2](#)

[30] Pratul P Srinivasan, Boyang Deng, Xiuming Zhang, Matthew Tancik, Ben Mildenhall, and Jonathan T Barron. Nerv: Neural reflectance and visibility fields for relighting and view synthesis. In *Proceedings of the IEEE/CVF Conference on Computer Vision and Pattern Recognition*, pages 7495–7504, 2021. [2](#)

[31] Cheng Sun, Min Sun, and Hwann-Tzong Chen. Direct voxel grid optimization: Super-fast convergence for radiance fields reconstruction. In *Proceedings of the IEEE/CVF Conference on Computer Vision and Pattern Recognition*, pages 5459–5469, 2022. [2](#)

[32] Towaki Takikawa, Alex Evans, Jonathan Tremblay, Thomas Müller, Morgan McGuire, Alec Jacobson, and Sanja Fidler. Variable bitrate neural fields. In *ACM SIGGRAPH 2022 Conference Proceedings*, pages 1–9, 2022. [2](#)

[33] Matthew Tancik, Pratul Srinivasan, Ben Mildenhall, Sara Fridovich-Keil, Nithin Raghavan, Utkarsh Singhal, Ravi Ramamoorthi, Jonathan Barron, and Ren Ng. Fourier features let networks learn high frequency functions in low dimensional domains. *Advances in Neural Information Processing Systems*, 33:7537–7547, 2020. [2](#)

[34] Shubham Tulsiani, Tinghui Zhou, Alexei A Efros, and Jitendra Malik. Multi-view supervision for single-view reconstruction via differentiable ray consistency. In *Proceedings of the IEEE conference on computer vision and pattern recognition*, pages 2626–2634, 2017. [3](#)

[35] Ali Osman Ulusoy, Andreas Geiger, and Michael J Black. Towards probabilistic volumetric reconstruction using ray potentials. In *2015 International Conference on 3D Vision*, pages 10–18. IEEE, 2015. [3](#)

[36] Dor Verbin, Peter Hedman, Ben Mildenhall, Todd Zickler, Jonathan T Barron, and Pratul P Srinivasan. Ref-nerf: Structured view-dependent appearance for neural radiance fields. In *2022 IEEE/CVF Conference on Computer Vision and Pattern Recognition (CVPR)*, pages 5481–5490. IEEE, 2022. [2](#)

[37] Jiepeng Wang, Peng Wang, Xiaoxiao Long, Christian Theobalt, Taku Komura, Lingjie Liu, and Wenping Wang. Neuris: Neural reconstruction of indoor scenes using normal priors. *arXiv preprint arXiv:2206.13597*, 2022. [1](#), [2](#), [3](#), [5](#), [6](#), [8](#)

[38] Peng Wang, Lingjie Liu, Yuan Liu, Christian Theobalt, Taku Komura, and Wenping Wang. Neus: Learning neural implicit surfaces by volume rendering for multi-view reconstruction. *arXiv preprint arXiv:2106.10689*, 2021. [1](#), [3](#), [4](#), [6](#), [8](#)

[39] Yi Wei, Shaohui Liu, Yongming Rao, Wang Zhao, Jiwen Lu, and Jie Zhou. Nerfingmvs: Guided optimization of neural radiance fields for indoor multi-view stereo. In *Proceedings of the IEEE/CVF International Conference on Computer Vision*, pages 5610–5619, 2021. [1](#), [3](#), [4](#), [6](#), [8](#)

[40] Qianyi Wu, Xian Liu, Yuedong Chen, Kejie Li, Chuanxia Zheng, Jianfei Cai, and Jianmin Zheng. Object-compositional neural implicit surfaces. *arXiv preprint arXiv:2207.09686*, 2022. [2](#), [3](#)

[41] Bangbang Yang, Yinda Zhang, Yinghao Xu, Yijin Li, Han Zhou, Hujun Bao, Guofeng Zhang, and Zhaopeng Cui. Learning object-compositional neural radiance field for editable scene rendering. In *Proceedings of the IEEE/CVF International Conference on Computer Vision*, pages 13779–13788, 2021. [2](#)

[42] Lior Yariv, Jiatao Gu, Yoni Kasten, and Yaron Lipman. Volume rendering of neural implicit surfaces. *Advances in Neural Information Processing Systems*, 34:4805–4815, 2021. [1](#), [2](#), [3](#), [4](#), [6](#), [8](#)

[43] Lior Yariv, Yoni Kasten, Dror Moran, Meirav Galun, Matan Atzmon, Basri Ronen, and Yaron Lipman. Multiview neural surface reconstruction by disentangling geometry and appearance. *Advances in Neural Information Processing Systems*, 33:2492–2502, 2020. [3](#)

[44] Zehao Yu, Songyou Peng, Michael Niemeyer, Torsten Sattler, and Andreas Geiger. Monosdf: Exploring monocular geometric cues for neural implicit surface reconstruction. *NeurIPS 2022*, 2022. [1](#), [2](#), [3](#), [5](#), [6](#), [8](#)

[45] Shuaifeng Zhi, Tristan Laidlow, Stefan Leutenegger, and Andrew J Davison. In-place scene labelling and understanding with implicit scene representation. In *Proceedings of the IEEE/CVF International Conference on Computer Vision*, pages 15838–15847, 2021. [3](#)